

Civil Engineering Journal

(E-ISSN: 2476-3055; ISSN: 2676-6957)

Vol. 11, No. 10, October, 2025



Geopolymer Mortars from Tuff Waste: A Circular Approach

Nelli Muradyan ¹, Arusyak Arzumanyan ¹, Marine Kalantaryan ^{1*}, Kristina Khachatryan ¹, Elisabetta Zendri ², Avetik Arzumanyan ¹

Received 15 July 2025; Revised 19 September 2025; Accepted 26 September 2025; Published 01 October 2025

Abstract

This study explores the potential use of volcanic tuff mining waste in geopolymer mortar formulations, aiming to enhance recycling and promote sustainable construction. Two filler-to-binder ratios (70/30 and 65/35) were developed using a geopolymer binder composed of tuff waste, dolomite powder, and sodium silicate. The mortars were subjected to heat treatments at 200, 350, 500, and 650°C for 8.5 hours. Compared to natural tuff (reference sample), water absorption decreased from 16.8% to 7.7%, with the lowest absorption observed in the 65/35 composition. Flexural strengths increased by 0.97% to 117.1%, and compressive strengths improved by 17.8% to 97.1%, reaching their maximum at 500°C; at 650°C, strengths declined due to water evaporation, shrinkage, and microcrack formation. Softening coefficients increased by over 10%, indicating enhanced resistance to water-induced softening. The study demonstrates that incorporating dolomite powder improves water resistance, while tuff waste serves effectively as both filler and binder component. Moreover, geopolymer mortars produce significantly lower CO₂ emissions (0.133 t/m³) compared to ordinary Portland cement mortars (0.415 t/m³), highlighting their environmental advantage. These results underscore the potential of tuff-based geopolymer mortars for sustainable construction applications.

Keywords: Volcanic Tuff Waste (VTW); Dolomite Powder; Geopolymer Mortar; Softening Coefficient; Emission Variables.

1. Introduction

Conventional concrete is the most widely utilized anthropogenic construction material globally, the production of which is one of the largest consumers of natural raw materials, significantly impacting the environment. This phenomenon is attributed to the fact that the primary component in mortar and concrete compositions is cement as a binder, and the production of the latter is associated with substantial carbon dioxide emissions. Consequently, the increasing awareness of the world economy's sustainable development and global warming issues has prompted the construction industry to investigate and identify novel binders to replace Portland cement [1-3]. For this purpose, the research and development of non-clinker hydraulic binders and geopolymers, which serve as alternatives to Portland cement, is a highly pertinent issue. These materials are obtained through alkaline processing of anthropogenic and natural raw materials, including thermal power plant ash, feldspar rocks, slag, volcanic rocks, sedimentary rock waste, and other sources [4, 5]. These materials possess distinctive technical-operational properties and are considered an effective means of utilizing mineral waste. Currently, the management of industrial waste presents a universal challenge and one of the most complex issues confronting contemporary society, particularly in relation to the recycling of rocks accumulated in mines over extended periods.

^{*} Corresponding author: kalantaryan.marine@nuaca.am





© 2025 by the authors. Licensee C.E.J, Tehran, Iran. This article is an open access article distributed under the terms and conditions of the Creative Commons Attribution (CC-BY) license (http://creativecommons.org/licenses/by/4.0/).

¹ Faculty of Construction, National University of Architecture and Construction of Armenia, Yerevan 0009, Armenia.

² Department of Environmental Sciences, Informatics and Statistics, Ca' Foscari University Venice, 30125 Venice, Italy,

Geopolymer mortars and concretes have the potential to effectively utilize rock waste, addressing a significant environmental problem related to its disposal. The technology used to produce geopolymers offers advantages over traditional Portland cement production, as it does not require a high-temperature calcination process and does not emit carbon dioxide from the breakdown of carbonate raw materials. Geopolymer production allows for the incorporation of various industrial wastes, leading to significantly lower energy consumption and carbon dioxide emissions compared to traditional cement production. Geopolymer mortar and concrete are considered effective solutions for reducing CO₂ emissions in the construction industry. Studies have shown that using these materials can reduce total CO₂ emissions by 9% to 60%. This reduction is achieved because geopolymer mortars and concretes utilize treated rock waste as a binder instead of cement [6, 7].

Recent review studies underscore the carbon and energy benefits associated with waste-derived geopolymers and elucidate industrial pathways for transforming various waste streams into construction materials. These reviews consistently demonstrate reductions in embodied carbon when waste precursors such as fly ash, slag, volcanic residues, and demolition waste are utilized, particularly when the use of activators and processing energy is minimized [8]. Carbon dioxide (CO₂) emission accounts for approximately 5-8% of total global emissions, as 1 ton of CO₂ is released into the atmosphere during the production of 1 ton of Portland cement [9, 10]. Furthermore, cement is the third most energy-intensive material after steel and aluminum, consuming approximately 7% of the energy utilized by industry worldwide [11]. According to Burduhos Nergis et al. [12], the process of obtaining geopolymer contributes to a significant reduction of global warming, emitting 169kg of CO₂/m³, whereas during the production of ordinary Portland cement, 306kg of CO₂/m³ is emitted into the atmosphere. Consequently, the production of geopolymer mortar and concrete is considered a potential novel alternative construction material [13] with comparatively low CO₂ emissions [14].

Geopolymers can be synthesized by treating volcanic rock with an alkali activator. Tuff, a type of volcanic rock and a commonly used building material, generates a significant amount of waste when extracted from mines. This makes it a suitable raw material for producing geopolymer mortar and concrete. By utilizing tuff waste in the production of geopolymer mortar, we can effectively address several environmental issues, including the management of large and hazardous rock waste deposits, air pollution, and the degradation of agricultural land. Recent experimental investigations have identified several viable methodologies for transforming volcanic-type waste materials into functional geopolymeric products. For instance, volcanic tuff or ignimbrite residues have been effectively combined with metakaolin or utilized as the primary precursor to produce mortars with compressive strengths appropriate for non-structural and semi-structural applications, contingent upon the activation and curing processes employed [15]. In other cases, volcanic tuff has been blended with blast furnace slag or iron powder waste to accelerate setting and improve early strength, thereby expanding its applicability in construction [16].

An analysis of the research [17-19] presented in scientific literature indicates that tuff wastes, owing to their chemical reactivity, can be incorporated into the production of geopolymer binders, cement-based artificial stone materials, mortars, and concretes, utilizing sodium silicate as an alkali activator. Composite binders were synthesized using tuff waste [5], dolomite, and sodium silicate. Test specimens with dimensions h=d=50mm were fabricated and subjected to thermal treatment at temperatures up to 200°C. Subsequently, the compressive strength was determined, revealing an increase of 8.3-39.7% compared to the compressive strength of natural tuff, with a softening coefficient ranging from 0.7 to 0.89. The relatively high softening coefficient of the resultant non-cement artificial stone materials can be attributed to the inclusion of dolomite in the processed mixtures, which functions as a component that enhances water resistance. According to the research analysis [7], tuff wastes were processed using filler-composite binder ratios of 75/25 and 70/30, along with water/solid mass ratios ranging from 0.10 to 0.12% to create cementless artificial stone compositions. After heat treatment at a maximum temperature of 200°C, the density of cementitious artificial stone materials increased by 10.5-39%, water absorption, which decreased by 2-2.5%, and compressive strength indicators, which increased by 15-30%, were determined with the same indicators of natural tuff stones.

These findings are consistent with recent experimental studies that have demonstrated enhanced density and decreased water absorption when volcanic wastes are subjected to alkali activation or combined with hydraulic byproducts such as blast furnace slag [16, 20]. Several authors have investigated the strength of samples made with geopolymer mixtures, which were cured at ambient temperatures as well as at heat curing temperatures ranging from 40° C to 90° C, with curing times between 24 to 72 hours. The studies found that samples cured with heat typically achieve better geopolymerization and result in greater strength. This is because the most intense reactions that contribute to the formation of the geopolymer structure occur at temperatures around $(90 \pm 5)^{\circ}$ C. Recent research on volcanic precursors supports this trend: heat curing (e.g., $60-80^{\circ}$ C for limited durations) frequently enhances early strength and decreases water absorption in tuff-based geopolymers. However, ambient curing strategies are actively being investigated to optimize field applicability and minimize processing energy [15].

As volcanic tuff waste can be utilized for the production of geopolymeric binders and artificial stone materials with superior physical and mechanical properties compared to natural tuff, this study aims to investigate the influence of different thermal treatments (200, 350, 500, and 650 °C) on the water absorption, flexural and compressive strengths, water resistance, and microstructure of geopolymer mortars. In particular, the research focuses on the effective utilization of waste generated during volcanic tuff extraction for the development of geopolymer-based mortars. The

incorporation of such waste materials into construction composites not only promotes efficient recycling strategies but also contributes to environmentally sustainable construction practices. To assess the performance of tuff-based geopolymer mortars, two filler-to-binder ratios (70/30 and 65/35) were examined. The geopolymer binder was synthesized using volcanic tuff waste, dolomite powder, and sodium silicate, offering a low-carbon and eco-friendly alternative to conventional cementitious systems.

2. Materials and Methods

2.1. Materials

2.1.1. VTW

In this study, tuff rock mining waste from Byurakan village in the Ashtarak region of the Republic of Armenia was utilized as raw material for producing geopolymer mortar. Figure 1 illustrates the mine, clearly showing the significant and hazardous accumulation of waste. There are approximately 100 such mines in the Republic of Armenia, and the waste generated from tuff stone mining presents major environmental challenges [21]. These mines have been in operation for decades, resulting in significant challenges related to waste management on a global scale due to the substantial volume of waste and the limited availability of landfill space. Tuff is a volcanic rock formed from volcanic eruptions. It exhibits numerous advantageous properties, including diverse colors, high compressive strength, durability, low density, thermal conductivity, ease of processing, acid resistance, and the ability to withstand high temperatures [6, 22]. These technical characteristics present numerous opportunities for extracting valuable geopolymer mortars from rock waste, particularly VTW.







Figure 1. Photos of VTW from the Byurakan mine and the geographic coordinates of the location: 40.337533, 44.284090

The chemical composition of tuff waste was examined according to standard [23] and the results are displayed in Table 1.

Table 1. Chemical properties of VTW

| Compound | SiO ₂ | TiO ₂ | Al ₂ O ₃ | Fe ₂ O ₃ | MgO | CaO | K ₂ O + Na ₂ O | SO_3 | Loss on ignition |
|-------------|------------------|------------------|--------------------------------|--------------------------------|------|------|---|--------|------------------|
| Content (%) | 63.27 | 0.76 | 17.48 | 4.20 | 1.56 | 3.68 | 6.88 | 0.33 | 1.84 |

Figure 2 presents the refined principal mineralogical composition obtained from X-ray diffraction analysis, whereas Figure 3 displays the results of differential thermal analysis (DTA). These tuffs contain a significant amount of amorphous volcanic glass phase, as seen in Figure 2. The DTA analysis revealed four endothermic effects (Figure 3), which were attributed to polymorphic variations in SiO₂ during heating. The first effect, occurring between 180°C and 270°C, is likely due to the polymorphic transformation of $\beta_{cristobalite} \rightarrow \alpha_{cristobalite}$. The second effect, observed between 490°C and 600°C, is due to the phase transformation of $\beta_{quartz} \rightarrow \alpha_{quartz}$, which occurs at 573°C. The third effect, observed between 873 and 893°C, is due to the transition of $\beta_{quartz} \rightarrow \alpha_{tridymite}$.

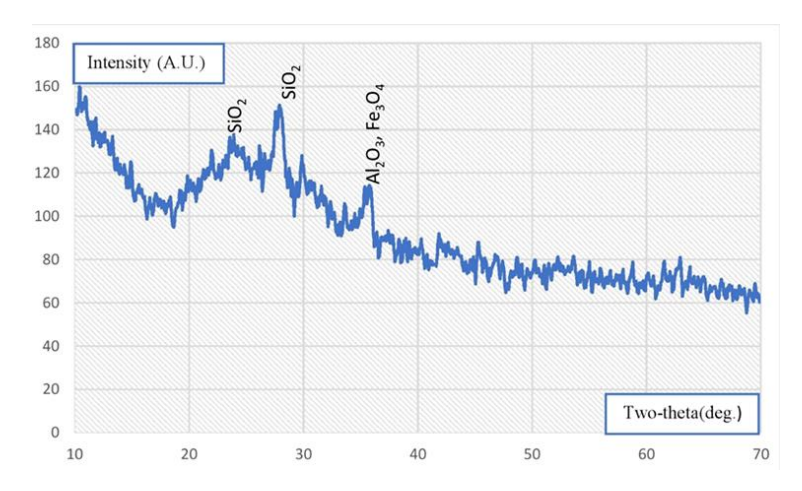


Figure 2. X-ray diffraction analysis of Tuff

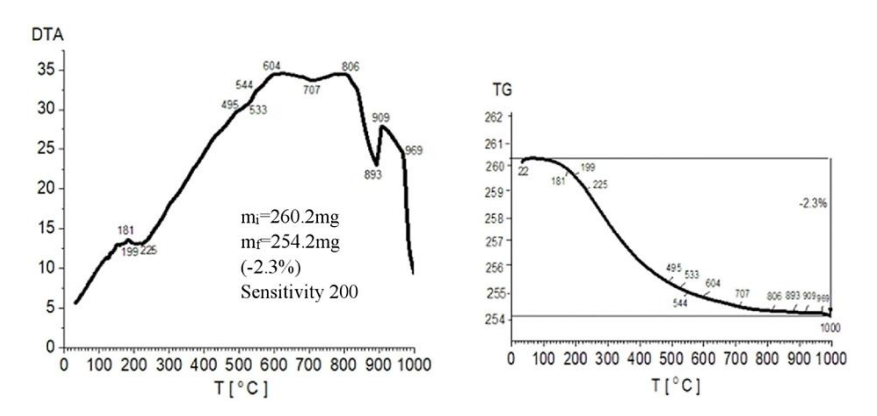


Figure 3. Differential Thermal Analysis of Tuff

The orange color of the rock is caused by the mineral Fe₂O₃, which was discovered by X-ray research. Fe₂O₃ is the result of magnetite oxidation. It also experiences polymorphic transition at 450-500°C: $\gamma_{Fe_{2O_3}} \rightarrow \alpha_{Fe_2O_3}$. The glass mass melts at 893°C and further recrystallization occurs. A 2.3% weight loss on the gravimetric curve (Figure 3) that is primarily observed at 220–250°C is likely caused by hydrated rocks (biotite and other such minerals) that are present in trace amounts in the Byurakan tuff and cannot be detected by X-ray diffraction analysis by subtracting hydrated water.

Figure 4 presents a scanning electron microscope (SEM) analysis of VTW at a magnification of 1000x. The analysis reveals that the majority of the tuff is made up of volcanic glass fragments, which can be found either densely packed or partially melted together. Additionally, some partial recrystallization of the glass is observed. Crystalline minerals are identified as plagioclase (Na,Ca)(Al,Si) [AlSi₂O₈] and broken grains of pyroxene.

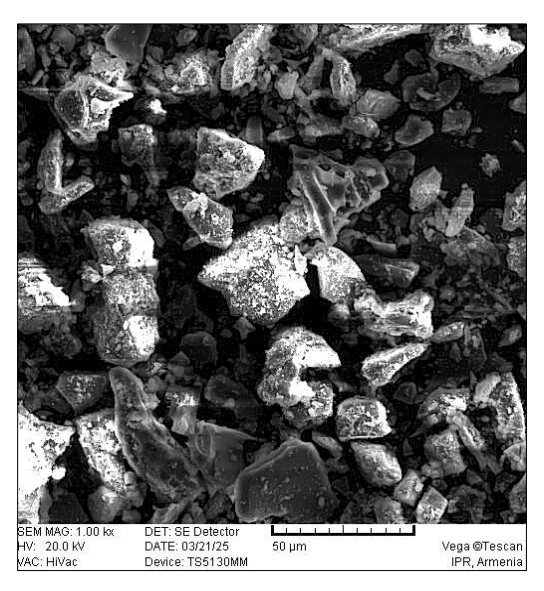


Figure 4. Scanning electron microscopy image of Tuff

2.1.2. Alkaline Activator

Sodium silicate undergoes hydration and hydrolysis to form a hydrogel consisting of silicon oxide and sodium hydroxide. This hydrogel interacts with the surface layer of active rock grains, in this case, VTW, binding them together to create a strong conglomerate mass. The use of sodium silicate as an alkaline activator in mortars and concretes ensures strength and durability. When sodium silicate reacts, it produces an aluminosilicate gel that can fill pores and microcracks, thereby enhancing strength and accelerating the healing process [24].

Sodium silicate (Na₂O·SiO₂) was used as an alkaline activator in the geopolymer mortars. The chemical and physical indicators of sodium silicate are presented in Table 2.

| Property | Unit | Results Obtained | | |
|--|--------------------|---------------------|--|--|
| SiO ₂ Na ₂ O Al ₂ O ₃ Fe ₂ O ₃ CaO Color Specific surface area | | 70.5 | | |
| Na ₂ O | | 24.8 | | |
| Al_2O_3 | content % | 2.1 | | |
| Fe_2O_3 | | 1.5 | | |
| CaO | | 70.5 24.8 2.1 | | |
| Color | - | white | | |
| Specific surface area | cm ² /g | 2750 | | |
| Silicate modulus | M_s | 2.8 | | |

Table 2. Physical and chemical properties of sodium silicate

2.1.3. Additive

Sodium silicate mixtures produce hydrate formations that are soluble in water. To mitigate their solubility, these mixtures are typically modified with various curing agents, such as acids, precipitation agents [18, 25, 26]. In this context, dolomite powder of sedimentary origin was incorporated as an additive to enhance the water resistance of the developed geopolymer mortars. Dolomite, an anhydrous carbonate sedimentary rock, primarily comprises calcium and magnesium carbonates (CaMg(CO)). While pure dolomite is white, the presence of iron and clay impurities can impart gray, yellow-gray, or greenish hues. Its crystal system is trigonal in structure [27, 28]. The chemical and physical properties of dolomite are presented in Table 3.

| Unit | Results Obtained | | |
|--------------------|---------------------------------|--|--|
| | 21. 9 | | |
| 0/ | 30. 3 | | |
| content % | 44.4 | | |
| | 3.4 | | |
| cm ² /g | 2700 | | |
| - | white | | |
| g/cm ³ | 2.82 | | |
| kg/m³ | 1670.5 | | |
| kg/m³ | 1825.4 | | |
| | content % cm²/g - g/cm³ kg/m³ | | |

Table 3. Physical and chemical properties of dolomite

2.1.4. Aggregates

Tuff waste from the Byurakan mine was utilized as a filler in geopolymer mortars after being sieved to produce sand. The grain composition of the sand in the formulated mixes is as follows: 35-37% in the 5.0-2.5 mm range, 12-14% in the 2.5-1.25 mm range, 16-18% in the 1.25-0.63 mm range, and 33-35% in the 0.63-0.315 mm range. The fundamental properties of the tuff sand, determined using standard testing procedures, are presented in Table 4 [29].

Table 4. Physical properties of tuff aggregates

| Property | Unit | Results Obtained |
|-------------------------------|-------------------|------------------|
| Bulk density | kg/m ³ | 1364 |
| Bulk density in compact state | kg/m^3 | 1567 |
| Water absorption (48 hour) | % | 22.7 |
| Fineness modulus | M_{f} | 2.9 |

2.2. Mixing and Sample Preparation

2.1.1. Geopolymer Binder

A geopolymer binder was prepared using specific materials. Tuff waste powder, with a particle size of less than 0.16 mm, served as the primary component. Dolomite powder, with a specific surface area of 2700cm²/g, was included as an additive. Sodium silicate, with a specific surface area of 2750cm²/g, was used as an alkaline activator. These raw materials were ground for 10 minutes using a laboratory ball mill (A091-02 Ball Milling Machine) to produce a geopolymer binder with a specific surface area ranging from 3100 to 3250cm²/g. Figure 5 illustrates the materials used in preparing the geopolymer binder, along with the raw materials required for its production. The specific surface area of the geopolymer binder components were determined according to the EN 196-6:2018 [30].



Figure 5. The raw materials for geopolymer binder

Several geopolymer binder compositions were developed, but analysis of the testing data identified the following as optimal: 50% VTW, 30% dolomite powder, and 20% sodium silicate.

2.2.2. Geopolymer Mortar and Sample Preparation

In the composition of geopolymer mortars, tuff sand was utilized as a filler, while the geopolymer binder functioned as the binding agent. The filler-to-binder ratio was 1:2.5 for the 70/30 composition and 1:1.8 for the 65/35 composition. The density of the fresh mortars ranged between 1200-1250kg/m³. The preparation of the geopolymer mortar involved the following procedure: the geopolymer binder was initially added to the tuff sand, and the mixture was subsequently homogenized using a mortar mixer (E095 Mortar Mixer) at a speed of 140rpm for 4 minutes. Prismatic test samples of 40 x 40 x 160mm were made.

Heat treatment was conducted following the regimen outlined in Figure 6. The initial step involved raising the temperature from 20°C to $(90 \pm 5)^{\circ}\text{C}$ over 2 hours. The samples were then held at this temperature for an additional 3 hours. Following this, the temperature was increased from $(90 \pm 5)^{\circ}\text{C}$ to 200°C (or up to 350°C , 500°C , and 650°C depending on the specific treatment) for 2 hours. The samples were maintained at the target temperature for 1.5 hours before being cooled to room temperature. The entire heat treatment process lasted a total of 8.5 hours.

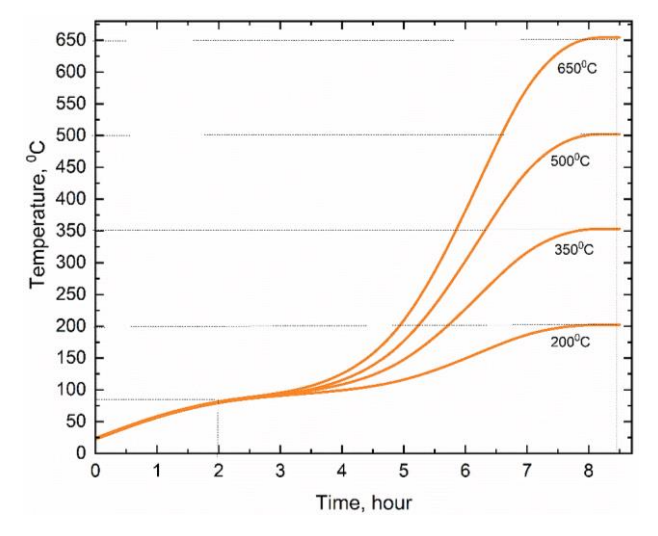


Figure 6. The mode used to thermally treat geopolymer mortars

Two geopolymer mortar compositions were developed with filler-to-geopolymer binder ratios of 70/30 and 65/35 by weight, using a fixed water-to-solid ratio of 0.25. The properties of the samples produced with these compositions - filler/geopolymer binder ratios of 65/35 and 70/30. The workflow of the methodology, including the raw materials used and the preparation and testing of samples, is presented in Figure 7.



Figure 7. Workflow of the methodology

The specimens formed from geopolymer mixtures prepared with the developed compositions are shown in Figure 8 after heat treatment. For comparison, tuff, a naturally occurring stone, is included as a reference material.

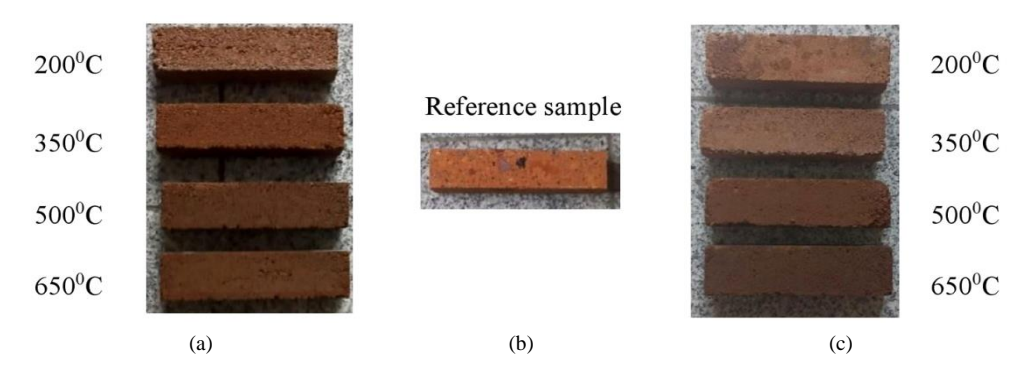


Figure 8. Geopolymer mortars 65/35 (a) and 70/30 (c) Filler/Geopolymer binders, natural stone (reference sample) (b)

2.3. Methods

2.3.1. Physical Characterization

The characteristics of geopolymer mortars were evaluated following a heat treatment of 8.5 hours and 28 days of storage under room conditions. The water absorption of geopolymer mortars was determined in accordance with the AST 100-94 [31] standard after 24 hours of water saturation of the test samples . The test samples were weighed using a scale with 0.1g accuracy (V073-01, Top loading balance $16 \text{ kg} \times 0.1 \text{ g}$, Matest, Italy).

2.3.2. Flexural Strength

The flexural strength of the specimen was evaluated using the standard testing procedure for geopolymer mortars, employing the Unitronic Compression/Tensile 50kN testing equipment, which has a maximum capacity of 50kN. The experiment was based on a three-point bending test conducted on a poured prism. A loading rate of 0.1kN/s (normative speed ranging from 0.1 to 0.2 kN/s) was applied to the specimen during the test. The hydraulic testing machine, which is controlled by a microprocessor, applies the load and is powered by a brushless motor with a closed-loop system that utilizes a camera encoder. To prevent unintentional manipulation of the machine, stroke electric end switches are installed on the load piston [32].

2.3.3. Compressive Strength

The compressive strength of geopolymer mortars was evaluated in accordance with the established standards [31]. Testing was conducted using an automated Servo-Plus Progress concrete compression machine, which has a capacity of 2000 kN and an accuracy of 0.001kN (Matest, Italy). The tests were performed at a 0.3MPa/s (normative speed ranging from 0.3 to 0.5 MPa/s). To determine the compressive strength, each test sample was weighed and measured in all dimensions. The lower support plate of the press was then positioned, and the upper support plate was smoothly lowered at the defined normative speed until the test specimen failed under the increasing compressive load (P).

2.3.4. Softening Coefficient

The softening coefficient of the tested samples was determined in accordance with the AST 100-94 standard (section 5.4) [31]. The tests assessed compression under both dry and immersed conditions. A pressure-driven press was used to conduct the tests, and the average results, Rw and Rd, were calculated for each batch.

2.3.5. Scanning Electron Microscopy (SEM)

A SE detector manufactured in the Czech Republic (VEGA TS 5130 MM "TESCAN") was used to analyze the microstructure of geopolymer mortars. For all SEM investigations, a high accelerating voltage of 14.0 kV was used.

3. Results and Discussion

Table 5 shows the physical and mechanical characteristics of geopolymers that have undergone heat-treated for 8.5 hours at 200, 350, 500, and 650°C utilizing filler/geopolymer binder compositions of 70/30 and 65/35. Indicators of the above characteristics of the reference sample, the tuff from the Byurakan mine, are also provided for comparison.

Table 5. Comparison of the mechanical and physical characteristics of Byurakan mine natural stone and geopolymer mortars developed from the same stone waste

| Samples | Filler/Geopolymer Binder % Ratio by Mass | Water/Solid Ratio | Average Density, kg/m³ | Water Absorption by Mass, % | Flexural Strength, MPa | Compression Strength, MPa | Softening Coefficient |
|-----------------------|---|----------------------|---------------------------|--------------------------------|---------------------------|------------------------------|--------------------------|
| Natural Tuff Stone | - | - | 1690 | 21.3 | 2.05 | 17.08 | 0.82 |
| GM_{200} | 70/30 | | 1968 | 16.8 | 2.07 | 20.12 | 0.82 |
| | 65/35 | | 1977 | 12.9 | 2.21 | 22.04 | 0.84 |
| GM_{350} | 70/30 | | 1960 | 16.4 | 3.19 | 24.41 | 0.84 |
| | 65/35 | 0.25 | 1989 | 10.8 | 3.38 | 25.63 | 0.89 |
| GM_{500} | 70/30 | 0.25 | 1967 | 14.9 | 3.91 | 30.08 | 0.91 |
| | 65/35 | | 1990 | 9.1 | 4.45 | 33.66 | 0.94 |
| GM_{650} | 70/30 | | 1962 | 13.3 | 3.66 | 28.27 | 0.88 |
| | 65/35 | | 1983 | 7.7 | 4.12 | 30.15 | 0.90 |

3.1. Water Absorption

To determine the water absorption of the geopolymer mortars, the test samples were first dried in a drying oven (mode I A007-04 KIT, Matest, Italy) at 105°C until a constant weight was achieved. After drying, the samples were weighed in air. Next, to ascertain the mass of the saturated test samples, they were submerged in a container filled with water at a temperature of (20±5)°C. The water level was maintained at least 50 mm above the upper mark of the test samples. Under these conditions, the samples were allowed to reach water saturation for a duration of up to (48) hours. After saturation, the samples were removed from the water, weighed in the air and continued the same process for another one hour. The test samples were considered water-saturated when the difference between the initial and final weighings did not exceed 0.2% [31].

Based on the water absorption data shown in Figure 9, the following conclusions can be made (the water absorption indicators of the geopolymer mortars were compared with the same indicators of the natural tuff: reference sample): the water absorption indicators of the GM200 samples were 16.8% for the 70/30 tuff sand/geopolymer binder composition and 12.9% for the case of 65/35. The water absorption indicators of GM350 test samples in the 70/30 composition were 16.4% and 65/35 were 10.8%. When the test samples were subjected to heat treatment at 500°C, the water absorption was 14.9% for GM500, 70/30 tuff sand/geopolymer binder composition, and 9.1% for 65/35. The water absorption indicators of the heat-treated samples at 650°C (GM650) were 13.3% for 70/30 and 7.7% for the 65/35 filler (tuff sand)/geopolymer binder composition. The water absorption of the natural tuff from the mine was 21.3%.

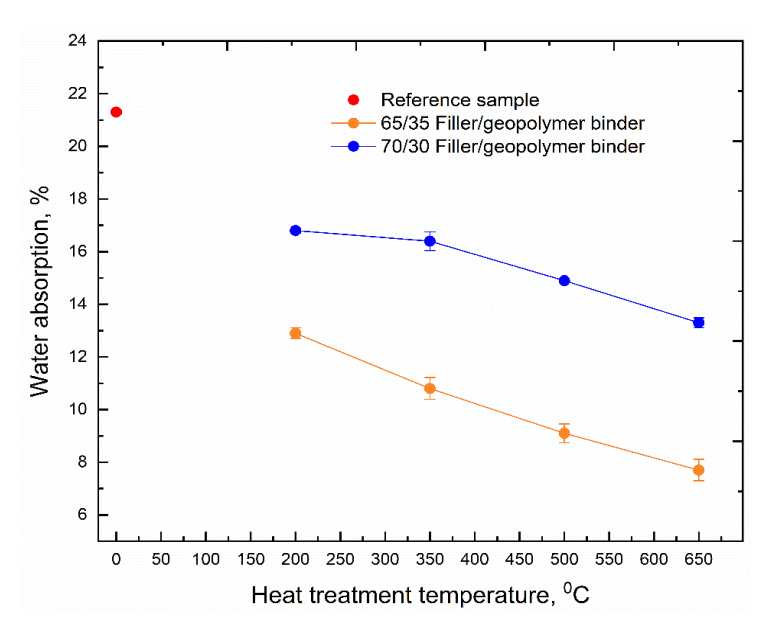


Figure 9. Results of water absorption for reference samples and the 65/35 and 70/30 Filler/Geopolymer binder samples at 28 days after heat treatment

Analyzing the obtained results, it is obvious that compared to the water absorption indicators of natural tuff stone, the water absorption indicator of processed geopolymer mortars decreased by 4.5-8% for the 70/30 composition, and 8.4-13.6% for the 65/35 composition. The observed decrease in water absorption with increased binder content and heat treatment signifies a densification of the matrix and a reduction in pore connectivity. These results indicate that the incorporation of volcanic tuff waste into geopolymer mortars not only enhances sustainability but also improves durability by reducing water uptake compared to natural tuff. Furthermore, the synergistic effects of a higher binder proportion and thermal treatment further contribute to the densification of the mortar microstructure [33].

3.2. Flexural Strength

Prismatic specimens measuring 40×40×160 mm composed of geopolymer mortars were tested to determine the flexural strength. The experimental procedure utilized a Unitronic Compression/Tensile 50kN compatible press (S337, Matest, Italy), applying a central single load to the test specimen [32]. The flexural strengths of geopolymer mortars prepared with 70/30 tuff sand/geopolymer binder composition were 2.07MPa for GM200, 3.19MPa for GM350, 3.91MPa for GM500 and 3.66MPa for GM650 (Figure 10). The bending strengths of the samples with 65/35 tuff sand/geopolymer binder composition and heat-treated at different temperatures were as follows: 2.21MPa for GM200, 3.38MPa for GM350, 4.45MPa for GM500, and 4.12MPa for GM650. All obtained flexural strength (Rfl) values were compared with the same value of natural tuff (reference sample), which was 2.05MPa.

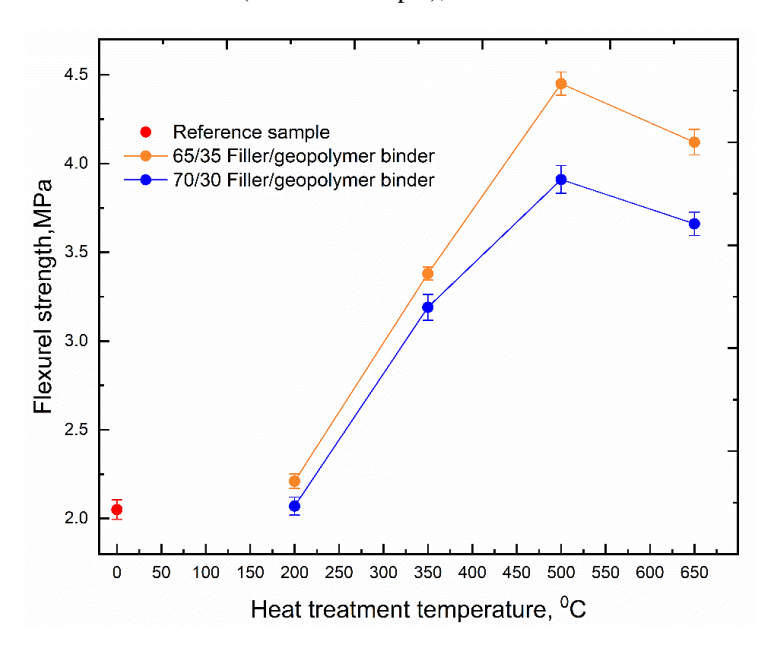


Figure 10. Results of Flexural strength for reference samples and the 65/35 and 70/30 Filler/Geopolymer binder samples at 28 days after heat treatment

Upon analysis of the flexural strength results for GM200, GM350, GM500, and GM650 geopolymer mortars presented in Figure 10, it is evident that the flexural strengths (Rfl) of samples produced with both 70/30 and 65/35 Filler/Geopolymer binder compositions demonstrated an increase of 1.5-2.2 times, relative to the corresponding property of the reference sample.

The findings suggest that an increase in the geopolymer binder fraction enhances the flexural strength of the mortars, likely due to a denser microstructure and stronger interfacial bonding between the binder gel and filler particles. Heat treatment further augmented strength up to 500°C, where the highest values were observed (3.91 MPa for 70/30 and 4.45 MPa for 65/35). At 650°C, a slight reduction was recorded, which may be attributed to microcracking induced by thermal stress [34].

3.3. Compressive Strength

The compressive strength was determined by testing cube-shaped test specimens with 40x40mm cross-sectional area of the test sample [31]. The compressive strengths of the test samples prepared with a 70/30 Filler/Geopolymer Binder mass ratio, heat treated at 200, 350, 500 and 650°C, and kept at ambient temperature for 28 days, were 20.12, 24.41, 30.08 and 28.27MPa, respectively, and in the case of 65/35: 22.04, 25.63, 33.66 and 30.15MPa (Figure 11).

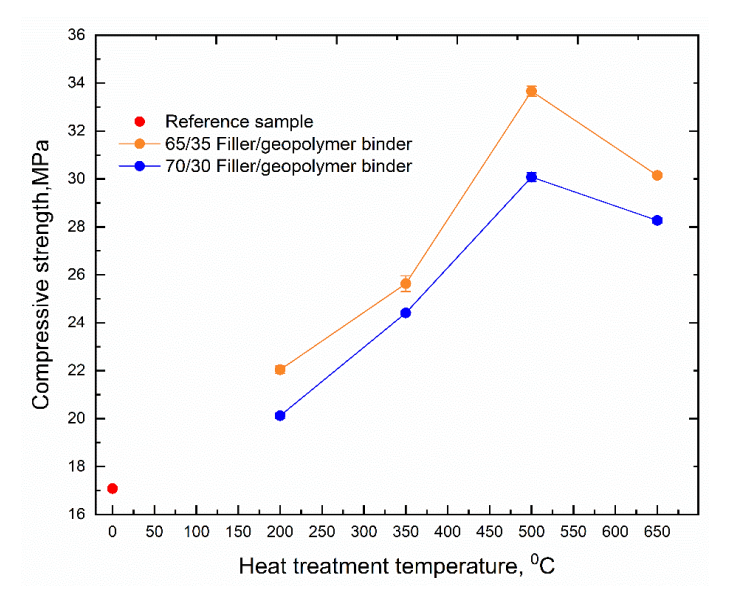


Figure 11. Results of Compressive strength for reference samples and the 65/35 and 70/30 Filler/Geopolymer binder samples at 28 days after heat treatment

The analysis of the data revealed that the strengths of the geopolymer mortars labeled GM200, GM350, GM500, and GM650 were 1.2 to 2 times greater than that of natural stone, which had a strength of 17.08MPa.

It is known from the literature that the use of up to 9% silicate glass in processed compositions leads to an increase in the strength of the final product. Otherwise, the adhesive contacts exceed the optimal amount, and the monolithic mortar or concrete mixture is transformed into a cohesive volumetric system, that is, the intergranular pore space of the material is almost filled with the adhesive and causes a decrease in strength [34-36]. A high silicate glass content is undesirable due to the formation of substantial quantities of alkali, which results in a significant deterioration of water resistance, compressive strength, and other critical operational properties of the final product. In the compositions of the geopolymer mortars developed in this study, silicate glass shards constitute 6-8% of the total mass of the mixture [37, 38].

The decrease in strength of the samples at 650°C, compared to those heat-treated at lower temperatures, can be explained by the fact that bound water in the geopolymer matrix starts to evaporate at higher temperatures. The loss of water can cause shrinkage and microcracking, leading to a reduction in compressive strength. Different components in the mortar, such as aggregates, sodium silicate, and the geopolymer matrix, may expand at different rates when exposed to high temperatures. This thermal expansion mismatch can induce internal stresses and microcracks, which weaken the overall structure [39].

3.4. Softening Coefficient

To determine the softening coefficient of the geopolymer mortars, half of the test samples made from the same batch were dried at 105°C until they reached a constant mass, and the other half were immersed in water and kept there for 1h at (20 ± 2) °C. These specimens were then tested under compression, and the average values of Rw and Rd were determined for each specimen. The ratio of the compressive strength limit of the water-saturated test sample Rw to the compressive strength limit in the dry state Rd is called the softening coefficient Ks [31, 40].

The softening coefficients (Ks) of the geopolymer mortars were determined and compared with those of the reference (tuff stone) sample, which are presented in Figure 12. The softening coefficients of the test samples prepared with 70/30 Filler/Geopolymer Binder composition, heat-treated at temperatures of 200, 350, 500 and 650° C and kept at ambient temperature for 28 days were 0.81, 0.84, 0.91, and 0.88, respectively, and in the case of 65/35 - 0.84, 0.89, 0.94 and 0.90. Reference sample Ks=0.82.

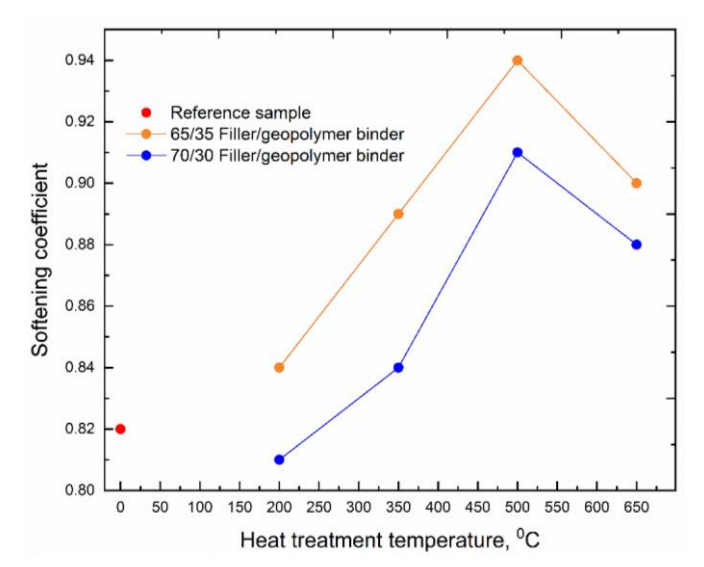


Figure 12. Results of Softening coefficient for reference samples and the 65/35 and 70/30 Filler/Geopolymer binder samples at 28 days after heat treatment

The findings demonstrate that an increase in the binder fraction leads to an enhancement of the softening coefficient, which aligns with the observed reduction in porosity and improved matrix densification. The highest value (Ks = 0.94) was recorded in the GM500 (65/35) composition, indicating excellent retention of compressive strength under water-saturated conditions. A slight reduction at 650°C can be attributed to microcracking induced by thermal stresses, akin to the behavior observed in compressive strength results [41]. The material is considered waterproof if Ks > 0.8 [5, 40]. Therefore, by analyzing the obtained results, which are also presented in Figure 12, it can be concluded that the developed geopolymer mortars are water resistant.

3.5. Scanning Electron Microscopy (SEM) Analysis

Scanning electron microscopy (SEM) studies were conducted on the geopolymer mortars obtained. The physical and mechanical properties of the specimens made with a 65/35 tuff sand and geopolymer binder composition and heat-treated at various temperatures were superior to those treated with a 70/30 composition. Consequently, SEM analyses were performed on the samples labeled GM200, GM350, GM500, and GM650, which utilized the 65/35 composition. Figure 13 presents SEM images at a 1000x magnification. The images correspond to (a) GM200, (b) GM350, (c) GM500, and (d) GM650.

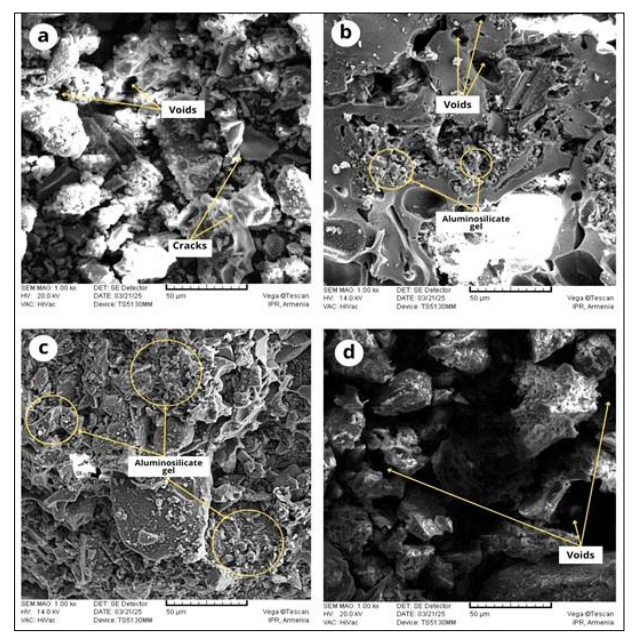


Figure 13. Microstructures of geopolymer mortar with alkali activator (GM200 - GM650:65/35 composition)

Figures 13-a and 13-d show the absence of a homogeneous matrix. In these images, voids, sediments, and cracks are present, indicating that the geopolymerization process has not been conducted optimally. Geopolymerization primarily occurs at the particle-liquid interface—that is, at the boundaries of the particles. The presence of sediments suggests that the reaction has terminated on the surfaces of the particles instead of fully interacting with all the tuff grains. This creates a layer that hinders the activation of the remaining particles, as the activators can only interact with the surface. Additionally, the structures formed display flat, plate-like surfaces. The pores and voids seen in Figure 13-d suggest that water bound in the matrix, formed at a relatively high temperature (650°C), has evaporated, leading to the development of this structure.

Figures 13-b and 13-c illustrate that a compact microstructure was formed in geopolymer mortars activated by alkali (sodium silicate) using volcanic tuff (VTW). In these samples, heat treatment was conducted at temperatures of 350°C and 500°C. The presence of Na₂O·SiO₂ enhances the dissolution of silicon and aluminum found in the volcanic tuff, which is crucial for developing a three-dimensional matrix structure [42-45]. Consequently, an aluminosilicate gel is created, which fills the voids within the matrix, resulting in a dense, amorphous structure. This process contributes to the improvement of the physicomechanical properties of the geopolymer mortars.

3.6. Emission Variables

The incorporation of mineral industrial waste - specifically, tuff and dolomite - in the production of geopolymer mortars enhances economic and environmental efficiency according to multiple criteria:

- By substituting primary raw materials with secondary ones, natural resource loss is minimized through complex utilization,
- Preventing environmental waste pollution during the extraction and processing of stone,
- Cultivating waste-filled lands is necessary to prevent damage caused by waste storage and maintenance costs.
 This involves implementing complex measures aimed at effectively restoring damaged lands and improving environmental conditions,
- Substituting Portland cement with a different geopolymer binder.

Ordinary Portland Cement Concrete (OPCC) is estimated to be utilized at a rate of one cubic meter per person per year globally rendering it one of the most consumed building materials after water [46]. Approximately 5% of global anthropogenic CO₂ emissions and 14% of the world's industrial energy consumption are linked to the production of ordinary Portland Cement (OPC) [47]. These emissions are largely driven by the energy-intensive manufacturing process and the calcination of limestone, which releases significant amounts of CO₂. OPC production exhibits high embodied energy consumption; consequently, each ton of OPC generates between 0.82 and 1.0 metric tons of CO₂ [48, 49]. A value of 0.84t-CO₂/t used in the calculations herein, is considered the worldwide average. On the other hand, aggregates require low energy for production compared to other materials, resulting in relatively low CO₂ emissions. The carbon dioxide (CO₂) emissions associated with the production of materials such as dolomite, alkali activators, tuff stone, and OPC vary significantly, primarily due to the differences in the manufacturing processes and the raw materials used. Approximately 0.7-0.9t of CO₂ per ton of cement produced, depending on the efficiency of the plant and the fuel type used. Dolomite (CaMg(CO₃)₂) has lower CO₂ emissions than OPC when used in construction. Dolomite production, primarily for use as aggregate or filler in construction, involves mining followed by minimal processing, such as crushing and grinding, resulting in CO_2 emissions of approximately 0.05–0.10 t per ton. These emissions depend on the energy required for extraction and processing. However, when dolomite is subjected to calcination (as in its use as a cementitious binder), the CO₂ emissions increase but remain lower than those associated with OPC [50].

Alkali-activated materials (AAMs), such as those used in geopolymers, use a chemical activator, like sodium hydroxide (NaOH) or sodium silicate to create a binding phase. The emissions depend on the specific activator used, with sodium silicate generally having higher emissions than sodium hydroxide due to the energy-intensive nature of its production. The emissions vary widely but are typically around 0.15-0.3t of CO_2 per ton of activator material, depending on the specific chemicals and their manufacturing processes. When combined with other precursors like fly ash or slag, the total CO_2 footprint can be much lower than OPC.

Tuff is a type of volcanic rock, and its usage in construction usually involves minimal processing (cutting and shaping). The emissions are primarily from the mining and transport stages. Around 0.10-0.50t of CO₂ per ton, depending on the energy used for extraction and transportation. It is much lower than OPC due to the absence of high-temperature processes [44]. For geopolymer mortars, incorporating dolomite, alkali activators, and tuff stone can significantly lower CO₂ emissions compared to traditional OPC-based mortars. The CO₂ emissions of two types of geopolymer mortars are presented in Figure 14: one activated with an alkaline activator (a) and the other incorporating OPC (b) [45, 51].

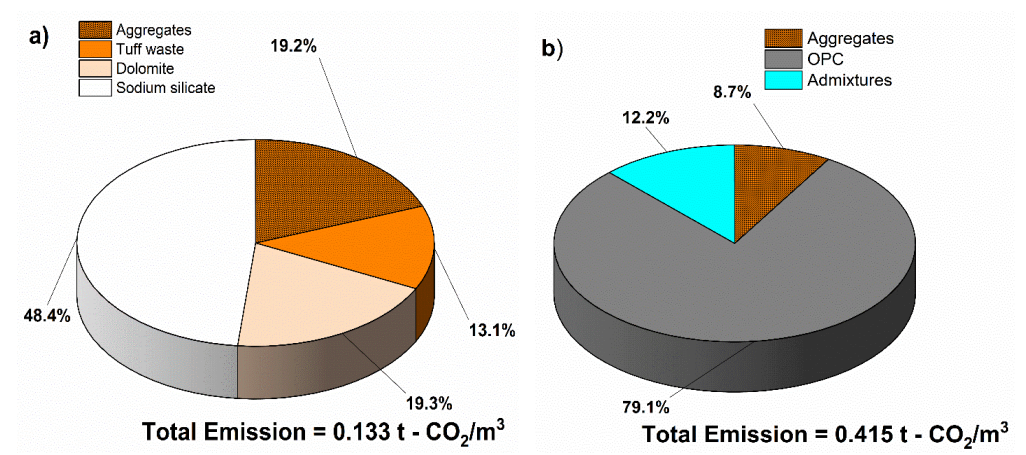


Figure 14. a) Geopolymer mortar with alkali activator (geopolymer binder) and b) mortar with OPC

Compared to mortars prepared with ordinary Portland cement, CO_2 emissions during the production of geopolymer mortars are significantly lower. The total emissions of geopolymer mortars are $0.133t - CO_2/m^3$ and OPC mortar $0.415t - CO_2/m^3$.

3.7. Comparison with Previous Studies

The results obtained in the present work for geopolymer mortars based on Byurakan tuff waste were compared with data from previous studies on similar aluminosilicate precursors. When compared with previous studies, our 28-day compressive strength results (reaching up to nearly double the reference sample) are higher than those reported for pumice-based mortars by Kabay et al. [52], who achieved 10–25 MPa under moderate thermal curing. They are also superior to volcanic tuff–BFS systems reported by Boumaza et al. [16], where compressive strength reached ~15 MPa under 80 °C curing. At the same time, our results approach the values obtained by Youssf et al. [53], who reported up to 50 MPa for construction and demolition waste-based mortars. Furthermore, unlike the decrease in strength observed by Khouadjia et al. [54] with iron powder fillers, the incorporation of dolomite powder in our compositions improved water resistance and maintained mechanical performance. Tekin et al. [55] also confirmed that introducing additional calcium-rich waste (travertine powder) enhanced strength, in line with the improvement we observed when dolomite was added.

Overall, the comparison demonstrates that Byurakan tuff-based geopolymer mortars exhibit competitive or superior performance compared to other volcanic tuff and pumice systems, while offering additional advantages such as lower water absorption and substantially reduced CO₂ emissions. This positions them as a sustainable alternative for construction and heritage restoration applications.

4. Conclusions

The urgent need for environmentally friendly building materials has driven research into sustainable alternatives to OPC. Geopolymer mortars from aluminosilicate materials offer improved mechanical and physical properties and lower CO₂ emissions. This work investigates the use of volcanic tuff mining waste as the main component in geopolymer mortars with an alkaline-activated binder, resulting in mortars with enhanced performance.

- Depending on the heat treatment temperature (GM200, GM350, GM500, GM650), water absorption of the samples varied with mix composition, ranging from 13.3% to 16.8% for the 70/30 composition, 7.7% to 14.9% for the 65/35 composition, and 21.3% for the control sample.
- Flexural strengths increased by 0.97% to 117.1% compared to the reference sample (natural tuff), depending on heat treatment.
- Compressive strength increased by 17.8% to 97.1% relative to the reference sample. At 650°C, strength decreased due to water evaporation in the geopolymer matrix, causing shrinkage and microcracks.
- Softening coefficients for 70/30 compounds were 0.82, 0.84, 0.91, and 0.88 (GM200–GM650), and for 65/35 compounds, 0.84, 0.89, 0.94, and 0.90, reflecting an increase of over 10%. This improvement indicates enhanced resistance to water-induced softening, which is important for maintaining long-term strength in wet conditions.
- Geopolymer mortars produce significantly lower CO₂ emissions than ordinary Portland cement mortars—approximately 0.133 t CO₂/m³ versus 0.415 t CO₂/m³—reducing emissions by more than threefold.

Highly reactive Armenian tuffs, especially their fine fractions, chemically interact with dolomite powder and alkali activators, enabling the development of building materials with improved properties, suitable for slabs, exterior and interior wall cladding, hollow blocks, cornices, planks, and other architectural or sculptural components.

5. Declarations

5.1. Author Contributions

Conceptualization, E.Z., N.M., M.K., K.K., Ar.Ar., and A.A.; methodology, N.M. and Ar.Ar.; software, Ar.Ar.; validation, M.K. and E.Z.; formal analysis, N.M. and E.Z.; investigation, N.M.; data curation, K.K.; writing—original draft preparation, N.M., K.K., and A.A.; writing—review and editing, M.K.; visualization, E.Z.; supervision, K.K.; funding acquisition, A.A. All authors have read and agreed to the published version of the manuscript.

5.2. Data Availability Statement

The data presented in this study are available on request from the corresponding author.

5.3. Funding and Acknowledgments

The authors would like to acknowledge the financial support of the Higher Education and Science Committee of the Republic of Armenia (Project No. 21AG-1C008), as well as from the RA state budget within the framework of the program "Maintenance and Development of the Research Laboratory of Construction and Architecture".

5.4. Conflicts of Interest

The authors declare no conflict of interest.

6. References

- [1] Nodehi, M., & Taghvaee, V. M. (2022). Alkali-Activated Materials and Geopolymer: a Review of Common Precursors and Activators Addressing Circular Economy. Circular Economy and Sustainability, 2(1), 165–196. doi:10.1007/s43615-021-00029-w.
- [2] Zaetang, Y., Wongkvanklom, A., Pangdaeng, S., Hanjitsuwan, S., Wongsa, A., Sata, V., & Chindaprasirt, P. (2025). Performance of Auto Glass Powder-High Calcium Fly Ash Geopolymer Mortar Exposed to High Temperature. Civil Engineering Journal (Iran), 11(6), 2343–2358. doi:10.28991/CEJ-2025-011-06-010.
- [3] Zou, H. Y., Zhong, W. L., Zhao, X., & Fan, L. F. (2024). Optimizing geopolymer mortar for shotcrete applications by focusing on flowability and early-age mechanical characteristics. Construction and Building Materials, 418, 135290. doi:10.1016/j.conbuildmat.2024.135290.
- [4] Liu, Y., Dong, B., Zhang, Y., Hou, D., & Wang, Y. (2024). Limestone powder-based alkali-activated materials: Influence of activator type. Powder Technology, 434, 119334. doi:10.1016/j.powtec.2023.119334.
- [5] Arzumanyan, A., & Muradyan, N. (2023). Development of composite binders based on volcanic tuff waste. International Journal of Applied Science and Engineering, 21(1), 2022347. doi:10.6703/IJASE.202403_21(1).004.
- [6] Henao Rios, L. M., Hoyos Triviño, A. F., Villaquirán-Caicedo, M. A., & de Gutiérrez, R. M. (2023). Effect of the use of waste glass (as precursor, and alkali activator) in the manufacture of geopolymer rendering mortars and architectural tiles. Construction and Building Materials, 363, 129760. doi:10.1016/j.conbuildmat.2022.129760.
- [7] Arzumanyan, A., Muradyan, N., Arzumanyan, A., Laroze, D., & Barseghyan, M. (2024). Non-Cement Building Materials from Volcanic Rock Extraction Waste. Buildings, 14(6), 1555. doi:10.3390/buildings14061555.
- [8] Kolade, A. S., Ikotun, B. D., & Oyejobi, D. O. (2025). Composition and performance driven mix design methodology for geopolymer mortars. Discover Civil Engineering, 2(1), 162. doi:10.1007/s44290-025-00327-4.
- [9] Davidovits, J. (2008). Geopolymer chemistry and applications. Geopolymer Institute. Saint-Quentin, France.
- [10] Huntzinger, D. N., & Eatmon, T. D. (2009). A life-cycle assessment of Portland cement manufacturing: comparing the traditional process with alternative technologies. Journal of Cleaner Production, 17(7), 668–675. doi:10.1016/j.jclepro.2008.04.007.
- [11] Gopalakrishnan, R., & Kaveri, R. (2021). Using graphene oxide to improve the mechanical and electrical properties of fiber-reinforced high-volume sugarcane bagasse ash cement mortar. European Physical Journal Plus, 136(2), 202. doi:10.1140/epjp/s13360-021-01179-4.
- [12] Burduhos Nergis, D. D., Abdullah, M. M. A. B., Vizureanu, P., & Mohd Tahir, M. F. (2018). Geopolymers and Their Uses: Review. IOP Conference Series: Materials Science and Engineering, 374(1), 12019. doi:10.1088/1757-899X/374/1/012019.
- [13] Shi, C., Jiménez, A. F., & Palomo, A. (2011). New cements for the 21st century: The pursuit of an alternative to Portland cement. Cement and Concrete Research, 41(7), 750–763. doi:10.1016/j.cemconres.2011.03.016.
- [14] McLellan, B. C., Williams, R. P., Lay, J., Van Riessen, A., & Corder, G. D. (2011). Costs and carbon emissions for geopolymer pastes in comparison to ordinary Portland cement. Journal of Cleaner Production, 19(9–10), 1080–1090. doi:10.1016/j.jclepro.2011.02.010.

[15] Morais, A. Í. S., Palmeira, D. K. O., Nascimento, A. M. D. S. S., Osajima, J. A., Garcia, R. R. P., & Huamán-Mamani, F. A. (2025). Development of Geopolymeric Mortar from Metakaolin and Ignimbrite from the Añashuayco Quarries, Peru, for Civil Construction. Sustainability (Switzerland), 17(13), 5714. doi:10.3390/su17135714.

- [16] Boumaza, A., Khouadjia, M. L. K., Isleem, H. F., Hamdi, O. M., & Khishe, M. (2025). Effect of blast furnace slag on the fresh and hardened properties of volcanic tuff-based geopolymer mortars. Scientific Reports, 15(1), 13651. doi:10.1038/s41598-025-98382-5.
- [17] Arzumanyan, A., Arzumanyan, A., & Muradyan, N. (2019). Heat-Acid-Resistant Light Concretes on the Base of Volcanic Tuff Lava and Pumice Aggregates of Armenia. Key Engineering Materials, 828, 141–145. doi:10.4028/www.scientific.net/kem.828.141.
- [18] Sahakyan, E., Arzumanyan, A., & Muradyan, N. (2022). Inorganic Polymeric Materials Based on Natural Silicate and Aluminosilicate Raw Materials. Key Engineering Materials, 906, 1–6. doi:10.4028/www.scientific.net/kem.906.1.
- [19] Sahakyan, E., Arzumanyan, A., & Muradyan, N. (2019). Physical and chemical processes of volcanic rock hardening with alkaline silicates. IOP Conference Series: Materials Science and Engineering, 698(2), 22078. doi:10.1088/1757-899X/698/2/022078.
- [20] Ekinci, E., Türkmen, İ., Kantarci, F., & Karakoç, M. B. (2019). The improvement of mechanical, physical and durability characteristics of volcanic tuff based geopolymer concrete by using nano silica, micro silica and Styrene-Butadiene Latex additives at different ratios. Construction and Building Materials, 201, 257-267. doi:10.1016/j.conbuildmat.2018.12.204.
- [21] SDA. (2025). Mining Industry in Armenia 2011. Research and Information Report: Armenian Development Agency, Yerevan, Armenia.
- [22] Galstyan, G., Arzumanyan, A., Tadevosyan, V., & Muradyan, N. (2023). Study of Stone Materials in "St. Astvatsatsin" Church of "Tatev" Monastery Complex. AIP Conference Proceedings, 2821(1), 0158656. doi:10.1063/5.0158656.
- [23] GOST 8269.1-97. (1997). Maintainous Rock Road-Metal and Gravel, Industrial Waste Products for Construction Works. Methods of Chemical Analysis. GOST, Moscow, Russia. Available online: https://files.stroyinf.ru/Index2/1/4294851/4294851516.htm (accessed on September 2025). (In Russian).
- [24] Yang, K. H., Song, J. K., Ashour, A. F., & Lee, E. T. (2008). Properties of cementless mortars activated by sodium silicate. Construction and Building Materials, 22(9), 1981–1989. doi:10.1016/j.conbuildmat.2007.07.003.
- [25] Chen, Y., Wang, X., Yu, C., Ding, J., Deng, C., & Zhu, H. (2019). Properties of inorganic high-temperature adhesive for high-temperature furnace connection. Ceramics International, 45(7), 8684–8689. doi:10.1016/j.ceramint.2019.01.190.
- [26] Davidovits, J. (2017). Geopolymers: Ceramic-like inorganic polymers. Journal of Ceramic Science and Technology, 8(3), 335–350. doi:10.4416/JCST2017-00038.
- [27] Mehmood, M. (2018). Dolomite and dolomitization model a short review. International Journal of Hydrology, 2(5), 549–553. doi:10.15406/ijh.2018.02.00124.
- [28] Warren, J. (2000). Dolomite: Occurence, evolution and economically important associations. Earth Science Reviews, 52(1–3), 1–81. doi:10.1016/S0012-8252(00)00022-2.
- [29] BS EN 1097-3:1998. (1998). Tests for mechanical and physical properties of aggregates Part 3: Determination of loose bulk density and voids. Bulgarian Institute for Standardization (BSI). London, United Kingdom.
- [30] EN 196-6:2018. (2018). Methods of Testing Cement Part 6: Determination of Fineness. European Committee for Standardization (CEN). Brussels, Belgium.
- [31] AST 100-94. (1995). Building Stones from Tuff, Basalt and Travertine: Specifications. Armstandard, Yerevan, Armenia.
- [32] EN 12372:2022. (2022). Natural Stone Test Methods Determination of Flexural Strength under Concentrated Load. European Committee for Standardization (CEN). Brussels, Belgium.
- [33] Ovbeniyekede, O. S., Adenan, D. S. Q. A., Ahmad, M., & Kamaruddin, K. (2018). Water Absorption and Compressive Strength of Self-Compacting Concrete Incorporating Fly Ash and Quarry Dust. International Journal of Scientific and Research Publications (IJSRP), 8(10), 8. doi:10.29322/ijsrp.8.10.2018.p8248.
- [34] Fernández-Jiménez, A., Palomo, A., Pastor, J. Y., & Martín, A. (2008). New cementitious materials based on alkali-activated fly ash: Performance at high temperatures. Journal of the American Ceramic Society, 91(10), 3308–3314. doi:10.1111/j.1551-2916.2008.02625.x.
- [35] Zawrah, M. F., Gado, R. A., Feltin, N., Ducourtieux, S., & Devoille, L. (2016). Recycling and utilization assessment of waste fired clay bricks (Grog) with granulated blast-furnace slag for geopolymer production. Process Safety and Environmental Protection, 103, 237–251. doi:10.1016/j.psep.2016.08.001.
- [36] Almalkawi, A. T., Hamadna, S., & Soroushian, P. (2017). One-part alkali activated cement based volcanic pumice. Construction and Building Materials, 152, 367-374. doi:10.1016/j.conbuildmat.2017.06.139.

[37] Mudgal, M., Singh, A., Chouhan, R. K., Acharya, A., & Srivastava, A. K. (2021). Fly ash red mud geopolymer with improved mechanical strength. Cleaner Engineering and Technology, 4, 100215. doi:10.1016/j.clet.2021.100215.

- [38] Diaz, E. I., Allouche, E. N., & Eklund, S. (2010). Factors affecting the suitability of fly ash as source material for geopolymers. Fuel, 89(5), 992–996. doi:10.1016/j.fuel.2009.09.012.
- [39] Chen, W., Li, B., Guo, M. Z., Wang, J., & Chen, Y. T. (2023). Impact of heat curing regime on the compressive strength and drying shrinkage of alkali-activated slag mortar. Developments in the Built Environment, 14, 100123. doi:10.1016/j.dibe.2023.100123.
- [40] AST EN 1469-2015 (2015). Natural stone products Slabs for cladding Requirements. Armstandard, Yerevan, Armenia.
- [41] Fernandez-Jimenez, A., García-Lodeiro, I., & Palomo, A. (2006). Durability of alkali-activated fly ash cementitious materials. Journal of Materials Science, 42(9), 3055–3065. doi:10.1007/s10853-006-0584-8.
- [42] Plando, F. R. P., Supnad, M. V., & Maquiling, J. T. (2025). Assessment of compressive strength, microstructure, thermal, and radiation shielding properties of Taal volcanic ash-based geopolymer mortar. Journal of Building Engineering, 99, 111572. doi:10.1016/j.jobe.2024.111572.
- [43] Gartner, E. (2004). Industrially interesting approaches to "low-CO2" cements. Cement and Concrete Research, 34(9), 1489–1498. doi:10.1016/j.cemconres.2004.01.021.
- [44] Yu, Z., Zhang, T., Deng, Y., Han, Y., Zhang, T., Hou, P., & Zhang, G. (2023). Microstructure and mechanical performance of alkali-activated tuff-based binders. Cement and Concrete Composites, 139, 105030. doi:10.1016/j.cemconcomp.2023.105030.
- [45] Wang, T., Fan, X., & Gao, C. (2024). Development of high-strength geopolymer mortar based on fly ash-slag: Correlational analysis of microstructural and mechanical properties and environmental assessment. Construction and Building Materials, 441, 137515. doi:10.1016/j.conbuildmat.2024.137515.
- [46] Saloni, Parveen, Lim, Y. Y., & Pham, T. M. (2021). Effective utilisation of ultrafine slag to improve mechanical and durability properties of recycled aggregates geopolymer concrete. Cleaner Engineering and Technology, 5, 100330. doi:10.1016/j.clet.2021.100330.
- [47] Thwe, E., Khatiwada, D., & Gasparatos, A. (2021). Life cycle assessment of a cement plant in Naypyitaw, Myanmar. Cleaner Environmental Systems, 2, 100007. doi:10.1016/j.cesys.2020.100007.
- [48] Hasanbeigi, A., Price, L., & Lin, E. (2012). Emerging energy-efficiency and CO2 emission-reduction technologies for cement and concrete production: A technical review. Renewable and Sustainable Energy Reviews, 16(8), 6220–6238. doi:10.1016/j.rser.2012.07.019.
- [49] Hills, T., Florin, N., & Fennell, P. S. (2016). Decarbonising the cement sector: A bottom-up model for optimising carbon capture application in the UK. Journal of Cleaner Production, 139(15), 1351–1361. doi:10.1016/j.jclepro.2016.08.129.
- [50] Sanjuán, M. Á., Andrade, C., Mora, P., & Zaragoza, A. (2020). Carbon dioxide uptake by cement-based materials: A Spanish case study. Applied Sciences (Switzerland), 10(1), 339. doi:10.3390/app10010339.
- [51] Abutaqa, A., Mohsen, M. O., Aburumman, M. O., Senouci, A., Taha, R., Maherzi, W., & Qtiashat, D. (2024). Eco-Sustainable Cement: Natural Volcanic Tuffs' Impact on Concrete Strength and Durability. Buildings, 14(9), 2902. doi:10.3390/buildings14092902.
- [52] Kabay, N., Mert, M., Miyan, N., & Omur, T. (2021). Pumice as Precursor in Geopolymer Paste and Mortar. Journal of Civil Engineering and Construction, 10(4), 225–236. doi:10.32732/jcec.2021.10.4.225.
- [53] Youssf, O., Safaa Eldin, D., & Tahwia, A. M. (2025). Eco-Friendly High-Strength Geopolymer Mortar from Construction and Demolition Wastes. Infrastructures, 10(4), 76. doi:10.3390/infrastructures10040076.
- [54] Khouadjia, M. L. K., Bensalem, S., Belebchouche, C., Boumaza, A., Hamlaoui, S., & Czarnecki, S. (2025). Sustainable Geopolymer Tuff Composites Utilizing Iron Powder Waste: Rheological and Mechanical Performance Evaluation. Sustainability (Switzerland), 17(3), 1240. doi:10.3390/su17031240.
- [55] Tekin, İ., Pekgöz, M., Dirikolu, İ., Valizadeh Kiamahalleh, M., Gholampour, A., Gencel, O., & Ozbakkaloglu, T. (2024). Effect of waste travertine powder on properties of rhyolitic tuff-based geopolymer. Journal of Building Engineering, 96, 108190. doi:10.1016/j.jobe.2024.110429.